MDPI

Article

Controlling Methane Ebullition Flux in Cascade Reservoirs of the Upper Yellow River by the Ratio of *mcrA* to *pmoA* Genes

Yi Wu [1,2], Xufeng Mao [1,2,*], Liang Xia [1,2], Wenjia Tang [3], Hongyan Yu [4], Ziping Zhang [3], Feng Xiao [5], Haichuan Ji [5] and Yuanjie Ma [5]

[1] Key Laboratory of Tibetan Plateau Land Surface Processes and Ecological Conservation (Ministry of Education), Qinghai Normal University, Xining 810008, China; mambawu@yeah.net (Y.W.); 15079266732@163.com (L.X.)

[2] School of Geographical Science, Academy of Plateau Science and Sustainability, Qinghai Normal University, Xining 810008, China

[3] State Key Laboratory for Environmental Protection Monitoring and Assessment of the Qinghai-Xining-Plateau, Xining 810007, China; qhtsy@126.com (W.T.); nxzhangjie@163.com (Z.Z.)

[4] Qinghai Qilian Mountain National Park Qinghai Service Guarantee Center, Xining 810008, China; qhyuhy@163.com

[5] Qinghai Forestry and Grass Bureau, Xining 810007, China; 13709760122@163.com (F.X.); jhcgryx@163.com (H.J.); mayuanjie2024@126.com (Y.M.)

* Correspondence: maoxufeng@yeah.net

Abstract: Reservoirs are an important source of methane (CH_4) emissions, but the relative contribution of CH_4 ebullition and diffusion fluxes to total fluxes has received little attention in the past. In this study, we systematically monitored the CH_4 fluxes of nine cascade reservoirs (Dahejia, Jishixia, Huangfeng, Suzhi, Kangyang, Zhiganglaka, Lijiaxia, Nina, and Longyangxia) in the upper reaches of the Yellow River in the dry (May 2023) and wet seasons (August 2023) using the static chamber gas chromatography and headspace equilibrium methods. We also simultaneously measured environmental physicochemical properties as well as the abundance of methanogens and methanotrophs in sediments. The results showed the following: (1) All reservoirs were sources of CH_4 emissions, with an average diffusion flux of 0.08 ± 0.05 mg m^{-2} h^{-1} and ebullition flux of 0.38 ± 0.41 mg m^{-2} h^{-1}. Ebullition flux accounted for $78.01 \pm 7.85\%$ of total flux. (2) Spatially, both CH_4 diffusion and ebullition fluxes increased from upstream to downstream. Temporally, CH_4 diffusion flux in the wet season (0.09 ± 0.06 mg m^{-2} h^{-1}) was slightly higher than that in the dry season (0.08 ± 0.04 mg m^{-2} h^{-1}), but CH_4 ebullition flux in the dry season (0.38 ± 0.48 mg m^{-2} h^{-1}) was higher than that in the wet season (0.32 ± 0.2 mg m^{-2} h^{-1}). (3) qPCR showed that methanogens (*mcrA* gene) were more abundant in the wet season ($5.43 \pm 3.94 \times 10^5$ copies g^{-1}) than that in the dry season ($3.74 \pm 1.34 \times 10^5$ copies g^{-1}). Methanotrophs (*pmoA* gene) also showed a similar trend with more abundance found in the wet season ($7 \pm 2.61 \times 10^5$ copies g^{-1}) than in the dry season ($1.47 \pm 0.92 \times 10^5$ copies g^{-1}. (4) Structural equation modeling revealed that the ratio of *mcrA*/*pmoA* genes, water N/P, and reservoir age were key factors affecting CH_4 ebullition flux. Variation partitioning further indicated that the ratio of *mcrA*/*pmoA* genes was the main factor causing the spatial variation in CH_4 ebullition flux, explaining 35.69% of its variation. This study not only reveals the characteristics and influencing factors of CH_4 emissions from cascade reservoirs on the Qinghai Plateau but also provides a scientific basis for calculating fluxes and developing global CH_4 reduction strategies for reservoirs.

Keywords: CH_4 flux; methanogen; methanotroph; Qinghai Plateau

1. Introduction

The construction of water reservoirs has significantly altered river channel morphology, hydrological conditions, and ecological environment, leading to changes in the nutrient

cycles of water bodies, land, and the atmosphere. The building of dams has resulted in a decrease in water flow velocity, causing suspended particles to settle in the reservoir. These sediments provide substrates (such as nitrogen and organic carbon) for the growth and reproduction of microorganisms and the generation of greenhouse gases in reservoirs [1]. Studies have found that damming can increase the emission of greenhouse gases (such as CH_4) from rivers compared to upstream sections [2,3]. CH_4 is the second most important greenhouse gas after carbon dioxide (CO_2), with a global warming potential (over a 100-year period) 25 times that of CO_2, contributing as much as 20% to global warming [4]. As one of the main components of greenhouse gases, the concentration of CH_4 in the atmosphere has been increasing at a rate of 7.6 ± 2.8 ppb per year since the Industrial Revolution. By 2022, the concentration of atmospheric CH_4 had reached 1923 ± 2 ppb, nearly three times higher than pre-industrial levels in 1750 [5]. CH_4 emissions are mainly released through three pathways: diffusion, bubbling (ebullition), and degassing. Currently, it is widely believed that downstream degassing is not the primary way of CH_4 emissions from reservoirs [6]. However, there is ongoing debate about whether diffusion or ebullition is the main emission pathway. Research on tropical eutrophic reservoirs has found that diffusion is the primary CH_4 emission pathway of the Eguzon reservoir, which has been in operation for nearly a century [7]. Conversely, an increasing number of studies indicate that CH_4 ebullition is the primary pathway in lakes, ponds, and rivers, contributing to over 80% of the total flux [8,9]. Research indicates that over 75% of future reservoir-induced radiative forcing will be generated by CH_4 ebullition and degassing flux [2]. Therefore, these flux pathways will be crucial for us to gain a deeper understanding and mitigate carbon emissions. Currently, the estimation of CH_4 emissions from most reservoirs is based solely on diffusion flux, leading to a significant increase in uncertainty in the estimation of CH_4 emissions from reservoirs. Therefore, there is an urgent need to conduct research on CH_4 ebullition from reservoirs.

Currently, cascade damming is widely adopted as a key technology to meet the needs of river water resources and the development and utilization of water energy resources. In the cascade development mode, the spatial distribution of reservoirs is relatively dense, and the longitudinal ecological elements of rivers exhibit characteristics that are significantly different from those of single-level reservoirs [10]. Therefore, the cumulative impact of cascade reservoirs on rivers is more complex than that of single-level reservoirs [11]. Previous studies have indicated that the construction of cascade reservoirs significantly increases the spatiotemporal heterogeneity of greenhouse gas emissions [12]. There is a significant increasing trend in emissions from upstream to downstream spatially. In the study of factors influencing CH_4 emissions in reservoirs, extensive research has been conducted on reservoir characteristics (such as location, construction time, hydraulic retention time, and reservoir area), climate characteristics (including temperature, precipitation, wind speed, and air pressure), sediment characteristics (such as organic matter and soil texture), and the physical and chemical properties of water bodies (nutrient elements, water temperature) [13,14]. However, CH_4 emissions in reservoirs are a complex biochemical process dynamically regulated by methanogenic and methanotrophic bacteria. These microorganisms play a key role in the production and consumption of CH_4 and are abundant in natural environments [15]. Currently, there is limited research on the correlation between CH_4 emission fluxes and methane-related microbial communities involved in methane metabolism, with most studies focusing on marine and freshwater lakes as well as rivers [16]. Further investigation is needed to explore the impact of methane-related microbial communities in reservoir sediments on CH_4 emissions.

The impact of global change on the Qinghai Plateau is significant and complex. An increasing number of studies indicate that the greenhouse gas emissions from water bodies on the plateau, especially from headwater rivers, are greater [17]. However, CH_4 emissions from reservoirs closely related to headwater rivers are often overlooked. It is increasingly recognized that assessing the spatial and temporal variability of CH_4 concentrations and emissions in hydropower reservoirs is crucial for accurate carbon budgets [18]. However,

there is limited research that simultaneously considers the spatiotemporal variability of CH_4 concentrations, fluxes, and methane-related microorganisms in these ecosystems [3,19]. Given the ongoing evolution of human activities and urbanization, the number of global reservoirs is increasing each year. In this study, we investigated the dissolved CH_4 concentration, diffusive flux, ebullition flux, and their driving factors in the cascade reservoirs of the upper Yellow River during an ice-free period in 2023. The study area is located on the Qinghai Plateau and represents a typical plateau cascade reservoir system. The objectives of this study were to (1) reveal the spatiotemporal heterogeneity of dissolved CH_4 concentration and fluxes, (2) investigate the contribution of CH_4 ebullition flux to the total flux, (3) explore the spatiotemporal distribution characteristics of relevant functional genes along the upper Yellow River, and (4) elucidate the key control factors of CH_4 fluxes.

2. Materials and Methods

2.1. Study Area and Sampling

The Yellow River, known as the mother river of China, originates from the northern foot of Bayan Har Mountains in the Qinghai Plateau and traverses the Qinghai Plateau, Loess Plateau, and North China Plain, with a total length of approximately 5464 km and a basin area of about 795,000 km^2, before flowing into the Bohai Sea. The upper reaches of the river basin, especially nine cascade reservoirs from Longyangxia to Dahejia, form an important water conservancy hub in the upper reaches of the Yellow River (Figure 1). From downstream to upstream, they are Dahejia (DHJ), Jishixia (JSX), Huangfeng (HF), Suzhi (SZ), Kangyang (KY), Zhiganglaka (ZGLK), Lijiaxia (LJX), Nina (NN), and Longyangxia (LYX). The long-term average flow rate in this area is about 600 m^3 s^{-1}. The long-term evolution of runoff shows an obvious alternation between abundance and scarcity. The extensive basin areas and steep terrain, particularly in its upper reaches, provide favorable conditions for hydroelectric development. From 1974 to 2015, these nine cascade reservoirs were successively built, forming a unique reservoir landscape in the upper reaches of the Yellow River. Among them, LYX and LJX are large reservoirs. These reservoirs not only serve multiple functions such as water regulation, supply, power generation, and flood control but also provide valuable field observation data for studying climate change, ecological environment, and greenhouse gas emissions in this region. They thus hold significant value for a deeper understanding of ecological changes within the upper reaches of the Yellow River Basin. Basic information on these reservoirs can be found in Table S1. The existence of these cascade reservoirs offers a rare research platform to explore relationship between greenhouse gas emissions and large-scale water conservancy projects. According to the 50 m interval from the dam, sampling work was conducted at six sampling points at LJX and LYX in May (dry season) and August (wet season) of 2023, with three sampling points at each of the remaining seven reservoirs. Water samples and sediment were collected at each sample point. Due to road collapse at LJX in August, sampling activities could not be carried out, resulting in missing data.

2.2. Sample Collection, Preservation, and Analysis

Portable water quality analyzer (HQ40d, Hach, CO, USA) was used to measure water temperature, dissolved oxygen (DO), salinity, and other data at each sampling point. The portable anemometer (Testo480, Lenzkirch, Germany) was used to measure wind speed. Water samples were collected using stainless steel samplers and stored in sample bottles for subsequent water quality index measurements. The detection indices include total nitrogen (TN), total phosphorus (TP), and total organic carbon (TOC), with detection methods mainly primarily following the protocols described by the State Environmental Protection Administration [20]. Surface sediments were collected at a depth of 0–10 cm using a sediment sampler. After thorough mixing of the sediments from all sampling points within each reservoir, a portion was placed into sealed bags for measuring physicochemical indicators (TN; TP; organic carbon, OC; pH), and another portion was transferred into 10 mL serum tubes. Samples were promptly transported to a portable refrigerator (TB5301,

Philips, Amsterdam, Netherlands), and upon return to the laboratory, the serum tubes were immediately stored at $-80\ ^{\circ}C$ for subsequent fluorescent quantitative PCR analysis of methane-related microorganisms.
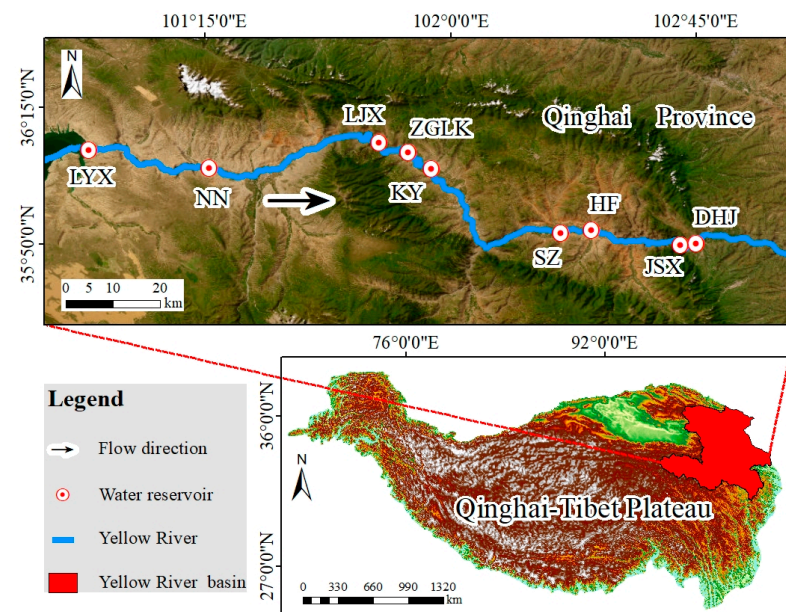
Figure 1. Distribution map of cascade reservoirs in the upper reaches of the Yellow River.

2.3. Collection and Calculation of CH$_4$

Total flux of CH$_4$ (F_{total}) is calculated using static chamber gas chromatography method [16], and the formula is as follows:

$$F_{total} = \frac{(N_t - N_0)}{At} \tag{1}$$

where N_t represents the concentration of CH$_4$ in the floating chamber at time t (min), N_0 represents the initial concentration of CH$_4$ in the floating chamber, and A (m^2) is the area between the floating chamber and the water surface.

CH$_4$ diffusion flux ($F_{diffusion}$) is calculated using the diffusion model [21], and the formula is as follows:

$$F_{diffusion} = K \times (C_{water} - C_{eq}) \tag{2}$$

where K (cm h^{-1}) represents the gas diffusion rate, C_{water} (µmol L^{-1}) is the dissolved concentration of CH$_4$ in the surface water, and CH$_4$ dissolved concentration is calculated using the headspace equilibrium method [22]. C_{eq} (µmol L^{-1}) is the concentration of CH$_4$ in water when reaching equilibrium between gas and liquid phases.

The ebullition flux of CH$_4$ ($F_{ebullition}$) is the difference between total flux and diffusion flux:

$$F_{ebullition} = F_{total} - F_{diffusion} \tag{3}$$

2.4. Extraction of DNA from Methane-Related Microorganisms and qPCR

Quantifications of *mcrA* and *pmoA* genes were quantified using quantitative PCR (qPCR) on the ABI 7300 Real-Time PCR system, following a previously reported method [23]. The *mcrA* gene was amplified using primer sets MLfF (5′-GGTGGTGTMGGATTCACACAR TAYGCWACAGC-3′) and MLfR (5′-TTCATTGCRTAGTTWGGRTAGTT-3′), resulting in a product length of approximately 471 bp. Similarly, the *pmoA* gene was amplified using primer sets A189F (5′-GGNGACTGGGACTTCTGG-3′) and mb661R (5′-CCGGMGCAACG TCYTTACC-3′) with a product length of approximately 509 bp. Triplicate PCR amplifications were carried out on an ABI 7300 Real-Time PCR system (ABI 7300, Applied

Biosystems, Foster City, CA, USA) in a total volume of 10 μL comprising 5 μL ChamQ SYBR Color qPCR Master Mix (2×), 0.4 μL each of forward and reverse primers (5 μM), 0.2 μL ROX Reference Dye 1 (5×), 1 μL DNA template, and 3 μL of ddH$_2$O. For *mcrA* and *pmoA* genes, the PCR thermocycling began at an initial denaturation step at 95 °C for 5 min, followed by 35 cycles consisting of melting at 95 °C for 30 s, annealing at 58 °C for 30 s, and extension at 72 °C for 1 min. Fluorescence data were collected after each cycle. Standard curves for *mcrA* and *pmoA* genes are y = −3.3311x + 38.689, R^2 = 0.9995 and y = −3.3622x + 39.685, and R^2 = 0.9945, respectively. The amplification efficiencies for *mcrA* and *pmoA* are 99.84% and 107.37%, respectively.

2.5. Statistical Analysis

A one-way analysis of variance was conducted using R 4.3.3 software to assess the impact of sampling reservoirs and seasons on environmental factors, dissolved CH$_4$ concentration, CH$_4$ fluxes, and methane-related microorganism gene abundance at a significance level of $p < 0.05$. In this study, the *piecewiseSEM* package (version 2.3.0) was employed to construct a structural equation model (SEM) using the *psem* command to assess the direct and indirect effects of environmental variables on CH$_4$ fluxes. The model hypothesis in this study was as follows: (1) reservoir properties may have influences on CH$_4$ fluxes. (2) environmental characteristics such as climate and sediment properties may indirectly influence CH$_4$ fluxes by impacting methanogenic and/or methanotrophic abundance. The *dredge* command in the *MuMIn* package (version 1.48.4) was used to simplify the models, and model comparison was conducted using the corrected Akaike information criterion (AIC). Given that the CH$_4$ flux at the water–air interface of the cascade reservoirs in the upper Yellow River is mainly contributed by CH$_4$ ebullition flux, we quantified the relative importance of methane-related microorganism gene abundance, reservoir properties, climatic characteristics, sediment, and water environment parameters on CH$_4$ ebullition flux using the *glmm.hp* command in the *glmm.hp* package (version 0.1–3) [24].

3. Results

### 3.1. Physical and Chemical Characteristics of Reservoirs

During the sampling period, the water temperature of the reservoir ranged from 6 to 16 °C, as shown in Figure S1. Spatially, along the flow direction, there was a general increasing trend in water temperature from 12.5 ± 2.5 °C at LYX to 28 ± 2.5 °C at DHJ (Figure S1). Wind speed ranged from 0.1 to 4.7 m s^{-1}, with significantly higher speeds in the dry season compared to the wet season. pH ranged from 7.75 to 8.78, with overall higher values in the dry season than in the wet season. TP showed an extremely high value of 0.36 mg L^{-1} in the dry season at DHJ and ranged from 0.01 to 0.02 mg L^{-1} elsewhere. TN was significantly higher in the dry season (1.18–11.48 mg L^{-1}) compared to the wet season (0.55–1.32 mg L^{-1}). TOC was significantly higher in the wet season (3.51–67.27 mg L^{-1}) compared to the dry season (0.01–38.8 mg L^{-1}).

The main physicochemical indicators of reservoir sediments are shown in Figure S2. pH ranges from 8 to 9.45, with significantly higher values in the dry season compared to the wet season and higher pH in the upstream reservoirs. TN ranges from 1.34 to 2.48 g kg^{-1}, showing noticeable seasonal fluctuations and regional differences without a clear pattern. TP ranges from 0.09 to 0.5 g kg^{-1}, with significantly higher values in the dry season compared to the wet season and higher TP in the upstream reservoirs in the dry season but lower values in the wet season. TOC ranges from 2.01 to 11.31 g kg^{-1}, showing large differences among reservoirs in the dry season, with higher TOC values in the middle reservoirs. However, differences are smaller in the wet season.

3.2. Spatiotemporal Distribution of Dissolved CH$_4$ Concentration

The characteristics of dissolved CH$_4$ concentration in nine reservoirs are shown in Figure 2, with all reservoirs acting as sources of CH$_4$ in both dry and wet seasons. Temporally, the dissolved CH$_4$ concentration in the Yellow River cascade reservoirs in the wet sea-

son (0.25 ± 0.14 μmol L^{-1}) was greater than that in the dry season (0.23 ± 0.15 μmol L^{-1}). Specifically, DHJ, HF, KY, ZGLK, NN, and LYX reservoirs all exhibited higher dissolved CH$_4$ concentrations in the wet season compared to the dry season, while JSX and SZ showed higher concentrations in the dry season than the wet season. Spatially, there was an increasing trend in dissolved CH$_4$ concentration from upstream (0.13 ± 0.06 μmol L^{-1}) to downstream (0.59 ± 0.01 μmol L^{-1}).
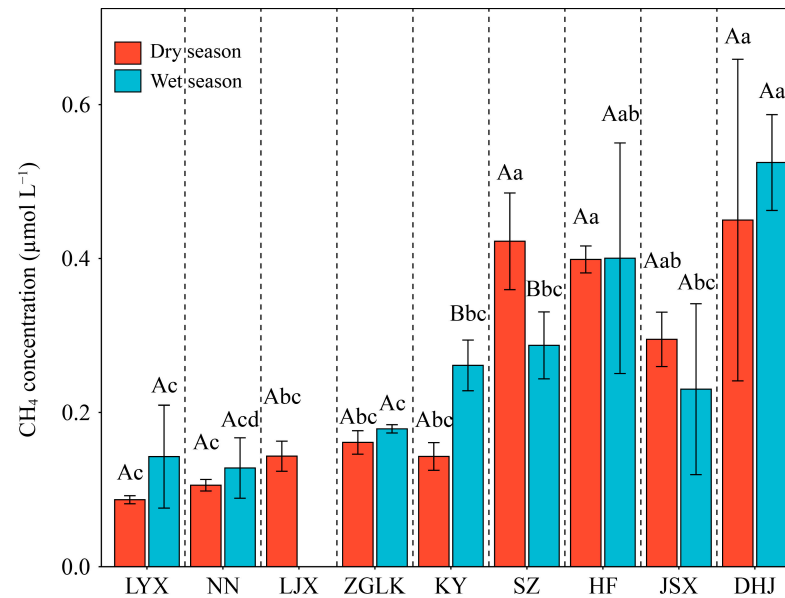
Figure 2. Temporal and spatial characteristics of dissolved CH$_4$ concentration at each reservoir along the upper Yellow River. Uppercase or lowercase letters indicate significant differences ($p < 0.05$) in gene abundance among nine cascade reservoirs in the same season or between two seasons within the same reservoir, respectively. Error bars represent standard deviations.
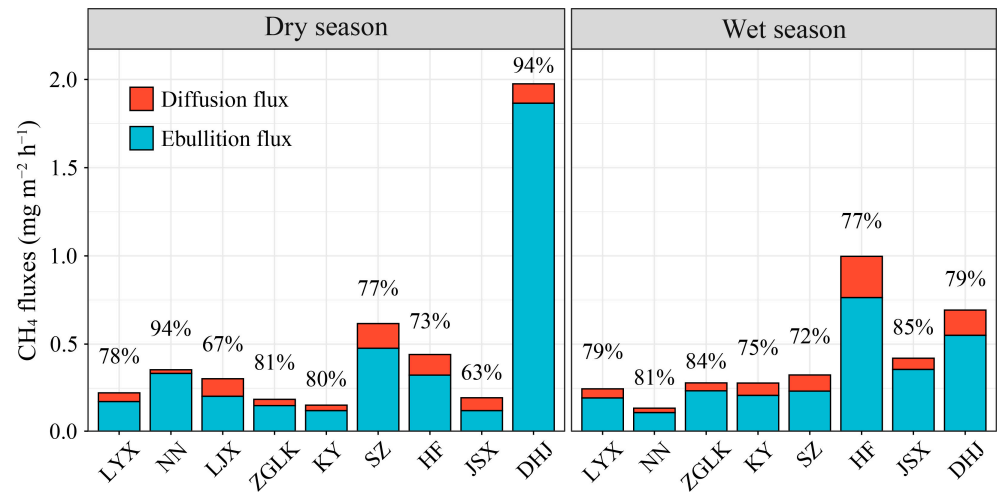
3.3. Spatiotemporal Characteristics of CH$_4$ Fluxes at the Water–Air Interface

During the observation period, the diffusion flux and ebullition flux of CH$_4$ in each reservoir and their proportions are shown in Figure 3. There is significant spatial variability in the two types of CH$_4$ fluxes among different reservoirs. Regardless of whether it is in the dry season or the wet season, each reservoir acted as a source of CH$_4$ and showed an increasing trend from upstream to downstream. Specifically, CH$_4$ diffusive fluxes in the wet season were higher than those in the dry season for DHJ, HF, KY, ZGLK, NN, and LYX reservoirs. Only JSX and SZ showed higher fluxes in the dry season than in the wet season. CH$_4$ diffusive fluxes of downstream reservoirs below 2000 m (DHJ, JSX, HF, and SZ) were significantly higher than those of the other five reservoirs above 2000 m ($p < 0.05$). CH$_4$ ebullition fluxes ranged from 0.01 to 3.91 mg m^{-2} h^{-1}. On a temporal scale, the mean ebullition fluxes in the dry season (0.39 ± 0.66 mg m^{-2} h^{-1}) were greater than those in the wet season (0.32 ± 0.26 mg m^{-2} h^{-1}). Spatially, CH$_4$ ebullition fluxes of downstream reservoirs below 2000 m (DHJ, JSX, HF, and SZ) were significantly higher than those of five upstream reservoirs above 2000 m ($p < 0.05$). The average contribution of ebullition flux to total flux for each reservoir was 73.83%, with a higher contribution in the dry season compared to that in the wet season ($p < 0.05$).

3.4. Spatiotemporal Changes in the Abundance of the mcrA and pmoA Genes

The abundance of the *mcrA* gene shows significant spatial heterogeneity among different reservoirs (Figure 4a). The copy numbers of the *mcrA* gene in nine reservoirs ranged from 6.29×10^3 to 1.38×10^6 copies g^{-1}, with higher abundance in the wet season ($5.4 \pm 3.94 \times 10^5$ copies g^{-1}) compared to the dry season ($3.74 \pm 1.34 \times 10^5$ copies g^{-1}). However, four reservoirs (SZ, KY, ZGLK, NN) exhibited higher *mcrA* gene abundance in

the dry season than in the wet season, and these four reservoirs are located in the middle and upper reaches of the cascade reservoir systems. In the dry season, the SZ and LJX reservoirs had the highest copy numbers of the *mcrA* gene at $5.79 \pm 1.51 \times 10^5$ copies g^{-1} and $5.74 \pm 0.45 \times 10^5$ copies g^{-1}, respectively, while the JSX, HF, and LYX reservoirs had copy numbers of the *mcrA* gene lower than 3×10^5 copies g^{-1}. In the wet season, the LJX reservoir had the highest copy number of the *mcrA* gene at $1.35 \pm 0.02 \times 10^6$ copies g^{-1}, which was also the highest among all reservoirs in both the dry and wet seasons. In contrast, the NN reservoir showed the minimum value with an *mcrA* gene copy number of only $9.62 \pm 3.65 \times 10^3$ copies g^{-1}.

Figure 3. Temporal and spatial characteristics of CH_4 ebullition and diffusion flux across the water–air interface in the cascade reservoirs along the upper Yellow River. The numbers on the column represent the contribution of ebullition flux to total flux.
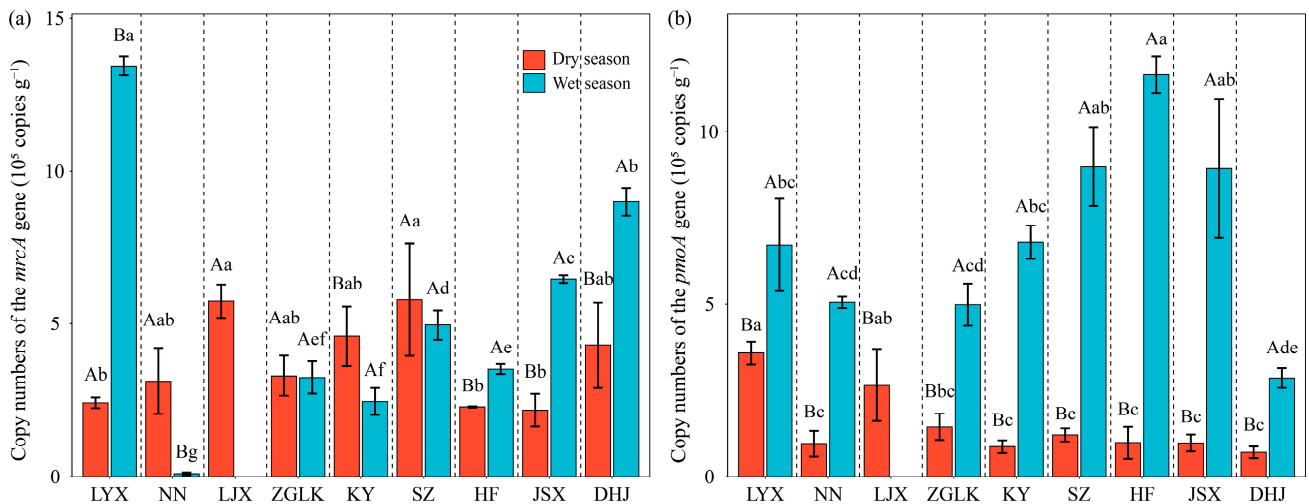

Figure 4. Copy numbers of the *mcrA* (**a**) and *pmoA* (**b**) genes from upstream to downstream (Longyangxia, LYX; Nina, NN; Lijiaxia, LJX; Zhiganglaka, ZGLK; Kangyang, KY; Suzhi, SZ; Huangfeng, HF; Jishixia, JSX; Dahejia, DHJ. Uppercase or lowercase letters indicate significant differences ($p < 0.05$) in gene abundance among nine cascade reservoirs in the same season or between two seasons within the same reservoir, respectively. Error bars represent standard deviations.

The abundance of the *pmoA* gene shows significant temporal heterogeneity among different seasons (Figure 4b). The copy numbers of the *pmoA* gene in nine reservoirs ranged from 4.99×10^4 to 1.22×10^6 copies g^{-1}, with all reservoirs exhibiting higher copy numbers in the wet season ($7 \pm 2.61 \times 10^5$ copies g^{-1}) compared to the dry season ($1.47 \pm 0.92 \times 10^5$ copies g^{-1}, $p < 0.01$). In the wet season, the reservoirs at JSX, HF, and SZ showed the highest copy numbers of the *pmoA* gene, with values of $8.95 \pm 1.65 \times 10^5$ copies g^{-1}, $1.17 \pm 0.04 \times 10^6$ copies g^{-1}, and $8.99 \pm 0.93 \times 10^5$ copies g^{-1}, respectively. In the dry season, LJX and LYX had the highest copy numbers of the *pmoA* gene among large reservoirs with values of 2.65×10^5 copies g^{-1} and 3.57×10^5 copies g^{-1}, respectively, while the other reservoirs had copy numbers below 2×10^5 copies g^{-1}.

3.5. Multiple Effects of Environmental Properties and Functional Microorganisms on CH$_4$ Ebullition Flux

Based on the field data, a structure equation model (SEM) was developed, incorporating physical and chemical properties of the water and sediment, reservoir characteristics, climate characteristics, and microbial abundance, as shown in Figure 5. The SEM in our study demonstrated a satisfactory fit to the data (Fisher's C = 41.01, $p = 0.68$, df = 23, AIC = 192.54) and accounted for approximately 83% and 54% of the variation in CH$_4$ ebullition and diffusion fluxes, respectively (Figure 5a). CH$_4$ ebullition flux was mainly influenced by reservoir area, sediment N/P, reservoir age, water N/P, water TOC, precipitation, and the *mcrA/pmoA*, which collectively explained 83% of the variation in CH$_4$ ebullition flux (Figure 5a). Reservoir area, sediment N/P, reservoir age, water N/P, and the *mcrA/pmoA* directly influenced CH$_4$ ebullition flux. Among these factors, the key driver of CH$_4$ ebullition flux was reservoir area (standard coefficient = 0.81), where CH$_4$ ebullition flux was significantly increased with reservoir area. The second most important factor was reservoir age (standard coefficient = −0.72). The magnitude of the water N/P effect (standard coefficient = −0.65) was comparable to that of the *mcrA/pmoA* (standard coefficient = 0.63) on CH$_4$ ebullition flux.
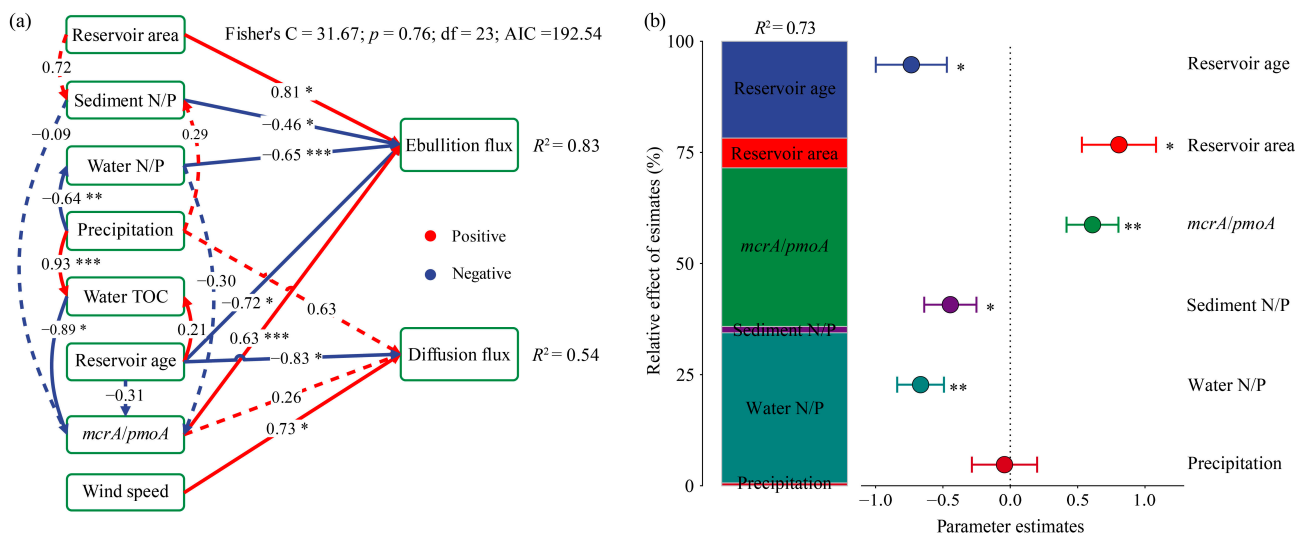
Figure 5. (**a**) The impacts of abiotic and biotic factors on CH$_4$ flux, both direct and indirect. The numbers above the arrows indicate path coefficients. The standardized direct and indirect effects of the environmental factors on CH$_4$ ebullition flux. (**b**) The rank of controlling factors. Solid lines represent statistical significance and dashed lines represent insignificance. All the asterisks denote significance (* $p < 0.05$; ** $p < 0.01$; *** $p < 0.001$).

Environmental factors can also indirectly influence the CH$_4$ ebullition flux by altering the *mcrA/pmoA*. Higher water TOC (standard coefficient = −0.89, $p < 0.05$) led to a decline in the *mcrA/pmoA*, which subsequently lowered CH$_4$ ebullition flux. Precipitation indirectly

decreased the CH_4 ebullition flux by affecting water TOC and the *mcrA/pmoA* with an indirect effect of 0.52. Collectively, reservoir area, reservoir age, precipitation, water TOC, sediment N/P, and water N/P accounted for 54% of the variance in the *mcrA/pmoA*. Furthermore, the results of the variation partitioning (Figure 5b) indicate that the key factors identified by SEM account for 84% of the variance in CH_4 ebullition flux. Specifically, 35.16% of this variance is attributed to the *mcrA/pmoA*, with water N/P (23.67%), reservoir age (20.87%), and reservoir area (8.39%) also emerging as important predictors.

4. Discussion

4.1. Ebullition Dominates the CH_4 Emissions from Cascade Reservoirs in the Upper Yellow River

During the sampling period, the surface water of the Yellow River cascade reservoirs remained highly saturated with CH_4. The mean CH_4 concentrations reached 1599% to 13,619% of atmospheric levels, indicating that the reservoirs were a significant source of atmospheric CH_4. This finding is consistent with observations in other inland aquatic ecosystems [9,25]. CH_4 diffusive flux estimated in this study (0.08 ± 0.07 mg m^{-2} h^{-1}) was lower than the average CH_4 diffusive flux in Chinese reservoirs (0.43 ± 1.39 mg m^{-2} h^{-1}) [26]. Total CH_4 diffusion and ebullition fluxes ranged from 0.08 to 4.18 mg m^{-2} h^{-1}, falling within the lower to moderate range of globally averaged fluxes for hydroelectric reservoirs (1.33–6.22 mg m^{-2} h^{-1}) [18]. Previous studies have focused less on CH_4 emissions from reservoirs in cold regions compared to those in tropical regions [27]. However, a comparison of CH_4 fluxes with other reservoirs (Table 1) shows that nine cascade reservoirs in this study, despite being located on the Qinghai Plateau, have significant CH_4 emissions. These fluxes are comparable to some tropical reservoirs and even exceed those of some temperate reservoirs. Compared to other reservoirs in the same region, CH_4 fluxes are also higher. These comparisons indicate that CH_4 emissions from cascade reservoirs in the upper reaches of the Yellow River cannot be ignored.

In most current CH_4 budget studies, total CH_4 emissions are typically represented only by CH_4 diffusion emissions, with little consideration given to the significance of CH_4 ebullition [28]. Bastviken et al. demonstrated that global freshwater ecosystems release 93.1 Tg of CH_4 annually, with approximately 59% (55.3 Tg CH_4) attributed to CH_4 ebullition [29]. In some extreme cases, CH_4 ebullition flux can exceed the diffusive flux by tens of times [30]. Previous research has indicated that younger reservoirs emit more CH_4 [2]. This relationship was also observed in nine cascade reservoirs in this study, with the youngest reservoir (DHJ, operational for 8 years) having the highest CH_4 emission flux (4.18 mg m^{-2} h^{-1}). Research on eutrophic old reservoirs in the tropics has shown that eutrophication promotes higher organic matter degradation, leading to increased CH_4 production. However, it has been found that diffusion flux is the primary emission pathway for CH_4 in such reservoirs (accounting for 78%) [7]. This may be mainly attributed to the fact that the reservoir has been constructed for nearly a century, and over its lifecycle, the potential for CH_4 emissions gradually decreases, resulting in insufficient CH_4 concentration in sediments to support bubble formation. Our study conducted the first measurement of CH_4 ebullition flux from cascade reservoirs in the upper Yellow River. The results revealed that ebullition is the primary pathway for CH_4 emissions in these reservoirs, with ebullition fluxes being two orders of magnitude higher than diffusion fluxes. Previous studies have indicated that reservoirs contribute the most to total CH_4 emissions among five major inland water bodies (rivers, reservoirs, lakes, ponds, and streams) [31]. Furthermore, research has shown that in high-latitude regions, CH_4 diffusion emissions are often inhibited due to low temperatures, low cumulative irradiance values, and short ice-free periods. As the cascade reservoirs in the upper Yellow River are located in a cold region, it is likely that CH_4 diffusion emissions are suppressed, leading to a higher contribution of CH_4 ebullition to the total flux [32].

**Table 1.** Comparison of CH_4 fluxes in different regions.

Reservoirs	Zones	Diffusion Flux (mg m^{-2} h^{-1})	Ebullition Flux (mg m^{-2} h^{-1})
Mekong River (China) [33]	tropic	0.18 ± 0.07	0.69 ± 0.69
Luanhe River Basin (China) [34]	temperate zone	0.04 ± 0.02	0.11 ± 0.04
Tana River (Kenya) [35]	tropic	0.08 ± 0.05	
Falling Creek Reservoir (America) [36]	temperate zone	0.27 ± 0.05	0.67 ± 0.31
Zangmu reservoir (China) [37]	Tibet Plateau	0.02	
This study	Qinghai Plateau	0.08 ± 0.05	0.38 ± 0.41

4.2. Spatiotemporal Characteristics of CH$_4$ Emissions from Cascade Reservoirs in the Upper Yellow River

CH_4 emissions from hydropower reservoirs exhibit significant spatial and temporal variability, with their magnitude varying by up to five orders of magnitude globally [18]. In this study, the diffusive fluxes from nine cascade reservoirs showed higher flux in the wet season compared to the dry season (Figure 3). Temperature and precipitation are widely recognized as two important factors influencing dissolved CH_4 concentration in aquatic ecosystems [38]. Due to the increased solar radiation, the air, water, and sediment temperatures in the wet season have significantly risen (Figure S1). The rise in environmental temperature will promote the metabolic activity of methanogens, subsequently increasing methane production rates [39]. At the same time, the solubility of methane in water decreases as water temperature increases, thereby further promoting the production and emission of CH_4 [40]. In addition, the increase in temperature can result in oxygen depletion, which subsequently promotes the accumulation of CH_4 by reducing CH_4 consumption. Previous studies have shown that precipitation has a dual effect on reservoirs. On the one hand, it increased the input of terrestrial organic matter and dissolved CH_4. On the other hand, it generates a dilution effect on dissolved CH_4 through increased runoff [41]. The higher dissolved CH_4 concentration in the wet season indicated that the dilution effect of precipitation is not significant on the dissolved CH_4 concentration in the cascade reservoirs of the Yellow River. This phenomenon may be attributed to the unique environmental conditions of the Qinghai Plateau. These lead to minimal changes in sediment properties between two seasons, while temperature exerts a more significant impact on methane-related microorganisms. As a result, hydraulic retention time has a relatively small effect. The observed CH_4 fluxes (diffusion and ebullition) exhibited greater variability in the dry season compared to the wet season (Figure 3). This is mainly due to the increased hydrological connectivity between the cascade reservoirs in the wet season, which enhanced the homogenization of dissolved CH_4 concentration and fluxes among different reservoirs. In the dry season, CH_4 ebullition flux was higher than that in the wet season. This phenomenon may be caused by changes in water level. Differences in water level can have a profound impact on CH_4 emission fluxes, with shallower water levels resulting in higher ebullition flux [42,43]. Spatially, the total CH_4 fluxes from upstream to downstream showed an increasing trend (Figure 3), which is similar to the findings of other studies on cascade reservoirs [44]. From the upstream to the downstream, temperature increased, and the wind speed decreased as altitude rapidly decreased. The enzymatic activity of sediment microorganisms in reservoirs increased with temperature, promoting substrate degradation and CO_2 production. This provided abundant substrates for hydrogenotrophic methanogens. Within a temperature range of 4–45 °C, the rate of CH_4 production is directly proportional to temperature [45].

4.3. The Ratio of the mcrA/pmoA Genes Affects CH$_4$ Ebullition Flux

CH$_4$ emissions depend on the balance between CH$_4$ production and consumption, which is closely linked to methane-related microorganisms. This process involves two types of microorganisms: methanogens and methanotrophs, both of which play a crucial role in the CH$_4$ cycle within ecosystems [15]. *mcrA* and *pmoA* are key functional genes for CH$_4$ production and oxidation, respectively [46]. Pearson's correlation analysis revealed no significant relationship between the abundance of the *mcrA* gene and environmental factors. In contrast, the abundance of the *pmoA* gene was found to be influenced by temperature and nutrient availability (Figure 6). SEM further demonstrated that the individual effects of the *mcrA* or *pmoA* gene abundance on CH$_4$ fluxes were not statistically significant. Instead, they exerted a negative effect on CH$_4$ ebullition flux through the ratio of the *mcrA/pmoA* genes (Figure 5). Variation partitioning revealed that the ratio of the *mcrA/pmoA* genes is a reliable predictor of CH$_4$ emissions. Since CH$_4$ is mainly produced in sediments, environmental factors indirectly affect CH$_4$ ebullition flux mainly by influencing the relative abundance ratio of two genes. Emerson et al. discovered that spatial variations in sediment microorganisms, especially those related to CH$_4$, can improve the precision of CH$_4$ emission estimation and prediction [47]. Research on rivers in the Qinghai Plateau has shown that sediment characteristics, organic substrate concentration, and the abundance of methanogens together explain 76% of CH$_4$ emissions [48].
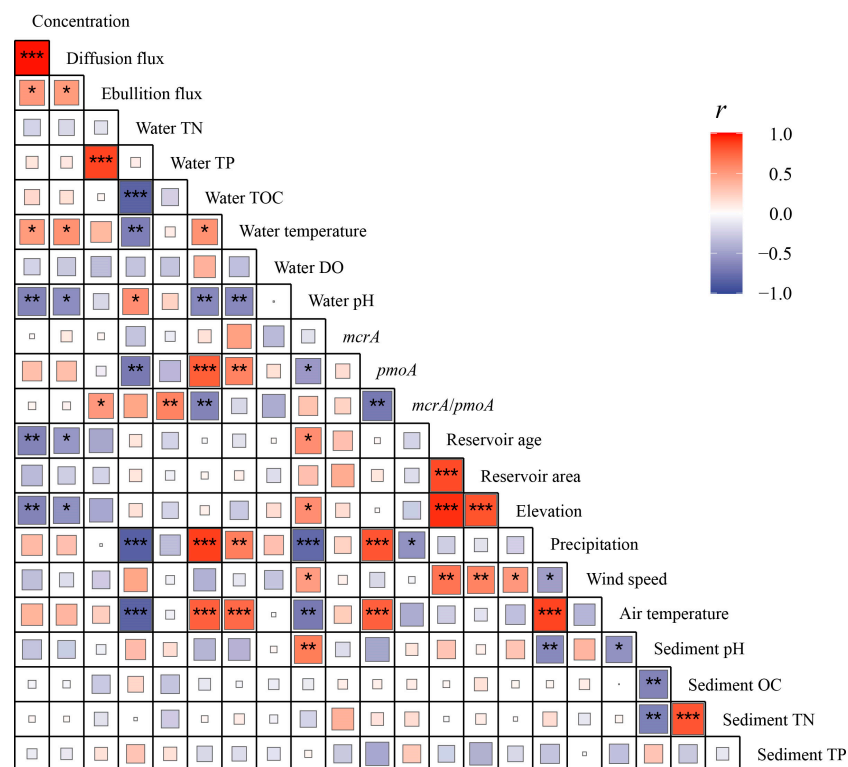
Figure 6. Relations between dissolved CH$_4$ concentration, fluxes, and environmental factors and functional gene abundance. The size of frames indicates the magnitude of the correlation between variables. All the asterisks denote significance (* $p < 0.05$; ** $p < 0.01$; *** $p < 0.001$).

Sediments can directly influence the CH$_4$ generation through their carbon, nitrogen, and phosphorus concentrations. In this study, we found a significant negative correlation between the CH$_4$ ebullition flux and the nitrogen/phosphorus concentration ratio ($p < 0.05$). A higher TP concentration can enhance the production of the CH$_4$ bubble, resulting in a greater proportion of ebullition flux [49]. Furthermore, changes in temperature and precipitation can indirectly impact CH$_4$ emissions by altering the substrate concentration required for CH$_4$ production. Organic carbon and nitrogen concentrations in the sediments

exhibited an increasing trend from upstream to downstream, following the direction of water flow (Figure S2). Concurrently, there was a gradual rise in water temperature as a result of decreasing elevation and the southward flow of water [50] (Figure S1). This change in temperature had an impact on the activities of methanogens and methanotrophs, leading to alterations not only in CH_4 fluxes but also in the relative contributions from different emission pathways. Research has shown that CH_4 emissions at the water–air interface primarily occur through ebullition when water temperature exceeds 11.7 °C, while diffusion is the main emission pathway below this threshold [51]. Wu et al. have demonstrated that combined with nitrogen addition, rainfall has a greater impact on CH_4 absorption compared to an increase in precipitation alone [52]. This may be due to the presence of sufficient nitrogen, which allows for the growth of methanotrophs in more humid conditions [53].

In addition to biotic factors, CH_4 emissions are closely related to abiotic factors such as the physicochemical properties of reservoir sediments and water, regional climate characteristics, etc. [2]. The relationship between dissolved CH_4 concentration and fluxes and environmental factors was shown in the heatmap based on Pearson's correlation analysis at *p*-values below 0.05 (Figure 6). In this study, a significant positive correlation was observed between the dissolved CH_4 concentration, diffusion, and ebullition flux. Conversely, the dissolved CH_4 concentration and diffusion flux showed a significant negative correlation with reservoir age, altitude, and water pH, while they exhibited a significant positive correlation with water temperature. However, the impact of reservoir area on CH_4 flux is not significant. This may be attributed to the location of the area on the Qinghai Plateau, which experiences a plateau semi-arid climate. This results in lower submerged biomass and organic carbon content in sediments compared to tropical reservoirs, as well as low water temperature. Additionally, human activities within the basin are relatively limited. These factors collectively contribute to a smaller influence of catchments on CH_4 flux. It is important to note that there is a highly significant positive correlation between the altitude and age of the cascade reservoirs in the upper reaches of the Yellow River ($p < 0.001$). Previous studies have shown that a gradual decrease in atmospheric pressure and temperature can result in a significant increase in CH_4 fluxes with increasing altitude in aquatic ecosystems [16]. However, it is important to note that this study did not find any significant impact of altitude on CH_4 ebullition flux. This could be due to the construction of cascade reservoirs along the upper reaches of the Yellow River, which were built successively from upstream to downstream, leading to a strong correlation between reservoir age and altitude (Figure 6). Consequently, the influence of reservoir age may have overshadowed the effect of altitude on CH_4 ebullition flux [54]. Alternatively, insignificant differences in altitude gradients within this study may also account for these findings. In this study, there is only a fall of approximately 800 m between the upstream and downstream reservoirs.

5. Conclusions

In recent years, there has been a significant focus on greenhouse gas emissions from hydropower reservoirs. With ongoing global changes, the uncertainty of greenhouse gas emissions from the Qinghai Plateau reservoirs, characterized by warming and increased humidity, has notably increased. In 2023, a comprehensive sampling effort was conducted at nine cascade reservoirs to evaluate CH_4 emissions from these reservoirs. This study examined the spatiotemporal patterns of CH_4 emissions in the densely dammed upper Yellow River, including dissolved concentration, ebullition, and diffusion fluxes. The main conclusions are as follows:

(1) The cascade reservoirs in the upper reaches of the Yellow River are a significant source of CH_4 emissions. Although located in an alpine region, their CH_4 emissions cannot be ignored, especially due to the high contribution of their ebullition fluxes. There is evident spatiotemporal heterogeneity in both dissolved CH_4 concentration and fluxes. Temporally, the diffusion flux of CH_4 is higher in the wet season compared to the dry season, while

the ebullition flux is higher in the dry season. Spatially, there is an increasing trend in both dissolved CH_4 concentration and fluxes from upstream to downstream.

(2) The abundance of the *mcrA* gene in the sediment of the cascade reservoirs in the upper Yellow River ranged from 6.29×10^3 to 1.38×10^6 copies g^{-1}, while the *pmoA* gene abundance ranged from 4.99×10^4 to 1.22×10^6 copies g^{-1}. Both *mcrA* and *pmoA* gene abundances were higher in the wet season compared to the dry season. Spatial differences were observed in the *mcrA* gene abundance, but no significant temporal variations were found. In contrast, the *pmoA* gene abundance exhibited significant temporal variations but not spatial differences.

(3) CH_4 emissions from cascade reservoirs are influenced by various factors, including the self-characteristics of the reservoirs, such as reservoir age and area; nutrient elements, such as total nitrogen and total phosphorus; and the abundance of methane-related functional genes. Among these factors, the ratio of the *mcrA/pmoA* genes explains 35.16% of the variation in CH_4 ebullition flux, while the water N/P, reservoir age, and reservoir area explain 23.67%, 20.87%, and 8.39%, respectively.

References

1. Maeck, A.; DelSontro, T.; McGinnis, D.F.; Fischer, H.; Flury, S.; Schmidt, M.; Fietzek, P.; Lorke, A. Sediment Trapping by Dams Creates Methane Emission Hot Spots. *Environ. Sci. Technol.* **2013**, *47*, 8130–8137. [CrossRef] [PubMed]
2. Soued, C.; Harrison, J.A.; Mercier-Blais, S.; Prairie, Y.T. Reservoir CO_2 and CH_4 emissions and their climate impact over the period 1900–2060. *Nat. Geosci.* **2022**, *15*, 700–705. [CrossRef]
3. Bai, X.X.; Xu, Q.; Li, H.; Cheng, C.; He, Q. Lack of methane hotspot in the upstream dam: Case study in a tributary of the Three Gorges Reservoir, China. *Sci. Total Environ.* **2020**, *754*, 142151. [CrossRef]
4. IPCC. Climate Change 2013: The Physical Science Basis. In *Working Group I Contribution to the Fifth Assessment Report of the Intergovernmental Panel on Climate Change*; Cambridge University Press: Cambridge, UK; New York, NY, USA, 2013.
5. WMO. *The State of Greenhouse Gases in the Atmosphere Based on Global Observations through 2022*; WMO: Geneva, Switzerland, 2023.
6. Grinham, A.; Dunbabin, M.; Albert, S. Importance of sediment organic matter to methane ebullition in a sub-tropical freshwater reservoir. *Sci. Total Environ.* **2018**, *621*, 1199–1207. [CrossRef]
7. Descloux, S.; Chanudet, V.; Serça, D.; Guérin, F. Methane and nitrous oxide annual emissions from an old eutrophic temperate reservoir. *Sci. Total Environ.* **2017**, *598*, 959–972. [CrossRef] [PubMed]
8. Zhang, L.; Zhang, S.; Xia, X.; Battin, T.J.; Liu, S.; Wang, Q.; Liu, R.; Yang, Z.; Ni, J.; Stanley, E.H. Unexpectedly minor nitrous oxide emissions from fluvial networks draining permafrost catchments of the East Qinghai-Tibet Plateau. *Nat. Commun.* **2022**, *13*, 950. [CrossRef]
9. Wang, L.; Du, Z.H.; Wei, Z.Q.; Xu, Q.; Feng, Y.R.; Lin, P.L.; Lin, J.H.; Chen, S.Y.; Qiao, Y.P.; Shi, J.Z.; et al. High methane emissions from thermokarst lakes on the Tibetan Plateau are largely attributed to ebullition fluxes. *Sci. Total Environ.* **2021**, *801*, 149692. [CrossRef] [PubMed]
10. Maavara, T.; Chen, Q.; Van Meter, K.; Brown, L.E.; Zhang, J.; Ni, J.; Zarfl, C. River dam impacts on biogeochemical cycling. *Nat. Rev. Earth Environ.* **2020**, *1*, 103–116. [CrossRef]

11. Ji, D.B.; Long, L.H.; Xu, H.; Liu, D.F.; Song, L.X. Advances in study on cumulative effects of construction of cascaded reservoirs on water environment. *Adv. Sci. Technol. Water Resour.* **2017**, *37*, 7–14. [CrossRef]

12. Shi, W.; Chen, Q.; Yi, Q.; Yu, J.; Ji, Y.; Hu, L.; Chen, Y. Carbon Emission from Cascade Reservoirs: Spatial Heterogeneity and Mechanisms. *Environ. Sci. Technol.* **2017**, *51*, 12175–12181. [CrossRef]

13. Beaulieu, J.J.; DelSontro, T.; Downing, J.A. Eutrophication will increase methane emissions from lakes and impoundments during the 21st century. *Nat. Commun.* **2019**, *10*, 1375. [CrossRef] [PubMed]

14. Isidorova, A.; Grasset, C.; Mendonça, R.; Sobek, S. Methane formation in tropical reservoirs predicted from sediment age and nitrogen. *Sci. Rep.* **2019**, *9*, 11017. [CrossRef] [PubMed]

15. Li, S.Q.; Zang, K.P.; Song, L. Review on methanogens and methanotrophs metabolised by methane in wetland. *Mar. Environ. Sci.* **2020**, *39*, 488–496. [CrossRef]

16. Zhang, L.W.; Xia, X.H.; Liu, S.D.; Zhang, S.B.; Li, S.L.; Wang, J.F.; Wang, G.Q.; Gao, H.; Zhang, Z.R.; Wang, Q.R.; et al. Significant methane ebullition from alpine permafrost rivers on the East Qinghai-Tibet Plateau. *Nat. Geosci.* **2020**, *13*, 349–354. [CrossRef]

17. Li, M.X.; Peng, C.H.; Zhang, K.R.; Xu, L.; Wang, J.M.; Yang, Y.; Li, P.; Liu, Z.L.; He, N.P. Headwater stream ecosystem: An important source of greenhouse gases to the atmosphere. *Water Res.* **2021**, *190*, 116738. [CrossRef]

18. Deemer, B.R.; Harrison, J.A.; Li, S.; Beaulieu, J.J.; DelSontro, T.; Barros, N.; Bezerra-Neto, J.F.; Powers, S.M.; dos Santos, M.A.; Vonk, J.A. Greenhouse Gas Emissions from Reservoir Water Surfaces: A New Global Synthesis. *Bioscience* **2016**, *66*, 949–964. [CrossRef]

19. Su, Y.M.; Liu, W.B.; Rahaman, M.H.; Chen, Z.B.; Zhai, J. Methane emission from water level fluctuation zone of the Three Gorges Reservoir: Seasonal variation and microbial mechanism. *Sci. Total Environ.* **2024**, *912*, 168935. [CrossRef]

20. State Environmental Protection Administration. *Methods for Water and Wastewater Monitoring and Analysis*; China Environmental Science Press: Beijing, China, 2002.

21. Wanninkhof, R. Relationship between wind speed and gas exchange over the ocean revisited. *Limnol. Oceanogr. Meth.* **2014**, *12*, 351–362. [CrossRef]

22. Johnson, K.M.; Hughes, J.E.; Donaghay, P.L.; Sieburth, J.M. Bottle-calibration static head space method for the determination of methane dissolved in seawater. *Anal. Chem.* **1990**, *62*, 2408–2412. [CrossRef]

23. Li, F.; Yang, G.; Peng, Y.; Wang, G.; Qin, S.; Song, Y.; Fang, K.; Wang, J.; Yu, J.; Liu, L.; et al. Warming effects on methane fluxes differ between two alpine grasslands with contrasting soil water status. *Agric. For. Meteorol.* **2020**, *290*, 107988. [CrossRef]

24. Lai, J.S.; Zou, Y.; Zhang, S.; Zhang, X.G.; Mao, L.F. glmm.hp: An R package for computing individual effect of predictors in generalized linear mixed models. *J. Plant Ecol.* **2022**, *15*, 1302–1307. [CrossRef]

25. Qin, Y.; Huang, H.; Li, Z.; Lu, L.H.; Tang, Q.; Su, Y.H.; Li, X.R. Research progress of aerobic methane oxidation process in inland waters. *J. Lake Sci.* **2021**, *33*, 1004–1017. [CrossRef]

26. Li, S.; Bush, R.T.; Santos, I.R.; Zhang, Q.; Song, K.; Mao, R.; Wen, Z.; Lu, X.X. Large greenhouse gases emissions from China's lakes and reservoirs. *Water Res.* **2018**, *147*, 13–24. [CrossRef]

27. Song, C.; Gardner, K.H.; Klein, S.J.; Souza, S.P.; Mo, W. Cradle-to-grave greenhouse gas emissions from dams in the United States of America. *Renew. Sustain. Energy Rev.* **2018**, *90*, 945–956. [CrossRef]

28. Zhang, P.; Wang, X.F.; Yuan, X.Z. General characteristics and research progress of methane emissions from freshwater ecosystems in China. *Chin. Environ. Sci.* **2020**, *40*, 3567–3579. [CrossRef]

29. Bastviken, D.; Tranvik, L.J.; Downing, J.A.; Crill, P.M.; Enrich-Prast, A. Freshwater Methane Emissions Offset the Continental Carbon Sink. *Science* **2011**, *331*, 50. [CrossRef] [PubMed]

30. Li, Z.; Zhang, C.; Liu, L.; Guo, J.S.; Fang, F.; Chen, Y.B. Ebullition fluxes of CO_2 and CH_4 in Pengxi River, Three Gorges Reservoir. *J. Lake Sci.* **2014**, *26*, 789–798. [CrossRef]

31. Zheng, Y.; Wu, S.; Xiao, S.; Yu, K.; Fang, X.; Xia, L.; Wang, J.; Liu, S.; Freeman, C.; Zou, J. Global methane and nitrous oxide emissions from inland waters and estuaries. *Glob. Change Biol.* **2022**, *28*, 4713–4725. [CrossRef] [PubMed]

32. Harrison, J.A.; Prairie, Y.T.; Mercier-Blais, S.; Soued, C. Year-2020 Global Distribution and Pathways of Reservoir Methane and Carbon Dioxide Emissions According to the Greenhouse Gas From Reservoirs (G-res) Model. *Glob. Biogeochem. Cycle* **2021**, *35*, e2020GB006888. [CrossRef]

33. Liu, L.; Yang, Z.; Delwiche, K.; Long, L.; Liu, J.; Liu, D.; Wang, C.; Bodmer, P.; Lorke, A. Spatial and temporal variability of methane emissions from cascading reservoirs in the Upper Mekong River. *Water Res.* **2020**, *186*, 116319. [CrossRef]

34. Yang, F.Y. The Study of Production, Emission and Influence Mechanism of Methane in Cascade Reservoirs of Luanhe River Basin. Master's Thesis, Northwest Normal University, Lanzhou, China, 2022.

35. Okuku, E.O.; Bouillon, S.; Tole, M.; Borges, A.V. Diffusive emissions of methane and nitrous oxide from a cascade of tropical hydropower reservoirs in Kenya. *Lakes Reserv. Res. Manag.* **2019**, *24*, 127–135. [CrossRef]

36. McClure, R.; Lofton, M.; Chen, S.; Krueger, K.; Little, J.; Carey, C. The magnitude and drivers of methane ebullition and diffusion vary on a longitudinal gradient in a small freshwater reservoir. *J. Geophys. Res. Biogeosci.* **2020**, *125*, e2019JG005205. [CrossRef]

37. Yang, M.; Hu, M.; Yang, T.; Zhang, L.; Wang, Q.; Yuan, S.; Ba, Z.; Xia, X. Greenhouse gas emissions from high-altitude hydropower reservoir: An example of the Zangmu reservoir on the Yarlung Tsangpo. *Acta Sci. Cirumstant.* **2022**, *42*, 188–194. [CrossRef]

38. Stanley, E.H.; Casson, N.J.; Christel, S.T.; Crawford, J.T.; Loken, L.C.; Oliver, S.K. The ecology of methane in streams and rivers: Patterns, controls, and global significance. *Ecol. Monogr.* **2016**, *86*, 146–171. [CrossRef]

39. Gudasz, C.; Bastviken, D.; Steger, K.; Premke, K.; Sobek, S.; Tranvik, L.J. Temperature-controlled organic carbon mineralization in lake sediments. *Nature* **2010**, *466*, 478–481. [CrossRef]

40. Pu, Y.N.; Jia, L.; Yang, S.J.; Qin, Z.H.; Su, R.M.Z.; Zhao, J.Y.; Zhang, M. The methane ebullition flux over algae zone of Lake Taihu. *Chin. Environ. Sci.* **2018**, *38*, 3914–3924. [CrossRef]

41. Wang, X.; He, Y.; Chen, H.; Yuan, X.; Peng, C.; Yue, J.; Zhang, Q.; Zhou, L. CH_4 concentrations and fluxes in a subtropical metropolitan river network: Watershed urbanization impacts and environmental controls. *Sci. Total Environ.* **2018**, *622–623*, 1079–1089. [CrossRef] [PubMed]

42. Saunois, M.; Stavert, A.R.; Poulter, B.; Bousquet, P.; Canadell, J.G.; Jackson, R.B.; Raymond, P.A.; Dlugokencky, E.J.; Houweling, S.; Patra, P.K. The global methane budget 2000–2017. *Earth Syst. Sci. Data* **2020**, *12*, 1561–1623. [CrossRef]

43. Harrison, J.A.; Deemer, B.R.; Birchfield, M.K.; O'Malley, M.T. Reservoir Water-Level Drawdowns Accelerate and Amplify Methane Emission. *Environ. Sci. Technol.* **2017**, *51*, 1267–1277. [CrossRef]

44. Tao, Y.C.; Fu, K.D.; Zhang, J.; Yang, L.S.; Yuan, X. Study on CO_2 and CH_4 emission fluxes from Lancang River cascade reservoirs. *Clim. Change Res.* **2024**, *20*, 107–117. [CrossRef]

45. Du, Q.Q.; Li, B.G.; Cai, H.M.; Deng, Y.; Wang, Y.C. Hydrochemical Characteristics of Cascade Reservoirs Waters along the Langcangjiang River and the Relative Influence on CO_2 Flux at Water/Air Interface. *Earth Environ.* **2023**, *51*, 36–46. [CrossRef]

46. Wen, P.; Tang, J.; Wang, Y.Q.; Liu, X.M.; Yu, Z.; Zhou, S.G. Hyperthermophilic composting significantly decreases methane emissions: Insights into the microbial mechanism. *Sci. Total Environ.* **2021**, *784*, 147179. [CrossRef] [PubMed]

47. Emerson, J.B.; Varner, R.K.; Wik, M.; Parks, D.H.; Neumann, R.B.; Johnson, J.E.; Singleton, C.M.; Woodcroft, B.J.; Tollerson, R.; Owusu-Dommey, A.; et al. Diverse sediment microbiota shape methane emission temperature sensitivity in Arctic lakes. *Nat. Commun.* **2021**, *12*, 5815. [CrossRef]

48. Liu, J.; Liu, S.D.; Chen, X.; Sun, S.Y.; Xin, Y.; Liu, L.; Xia, X.H. Strong CH_4 emissions modulated by hydrology and bed sediment properties in Qinghai-Tibetan Plateau rivers. *J. Hydrol.* **2023**, *617*, 129053. [CrossRef]

49. DelSontro, T.; Boutet, L.; St-Pierre, A.; del Giorgio, P.A.; Prairie, Y.T. Methane ebullition and diffusion from northern ponds and lakes regulated by the interaction between temperature and system productivity. *Limnol. Oceanogr.* **2016**, *61*, S62–S77. [CrossRef]

50. Ren, L.; Song, C.; Wu, W.; Guo, M.; Zhou, X. Reservoir effects on the variations of the water temperature in the upper Yellow River, China, using principal component analysis. *J. Environ. Manag.* **2020**, *262*, 110339. [CrossRef]

51. Ren, Y.J.; Deng, Z.M.; Xie, Y.H.; Zhu, L.L.; Chen, X.R.; Zhang, C.Y.; Chen, X.S.; Li, F.; Zhou, Y.A. Estimation of methane diffusion and ebullition flux and water environmental controls during flooding period in Lake Dongting wetlands. *J. Lake Sci.* **2019**, *31*, 1075–1087. [CrossRef]

52. Wu, H.; Wang, X.; Ganjurjav, H.; Hu, G.; Qin, X.; Gao, Q. Effects of increased precipitation combined with nitrogen addition and increased temperature on methane fluxes in alpine meadows of the Tibetan Plateau. *Sci. Total Environ.* **2020**, *705*, 135818. [CrossRef]

53. Bodelier, P.L.E.; Laanbroek, H.J. Nitrogen as a regulatory factor of methane oxidation in soils and sediments. *FEMS Microbiol. Ecol.* **2004**, *47*, 265–277. [CrossRef]

54. Barros, N.; Cole, J.J.; Tranvik, L.J.; Prairie, Y.T.; Bastviken, D.; Huszar, V.L.M.; del Giorgio, P.; Roland, F. Carbon emission from hydroelectric reservoirs linked to reservoir age and latitude. *Nat. Geosci.* **2011**, *4*, 593–596. [CrossRef]